

INFLUENCE OF INTERNAL STRESSES ON THE DEVELOPMENT OF CRACKS  
IN GLASSES

U. Soltész, H. Richter and E. Sommer

Fraunhofer-Institut für Werkstoffmechanik  
Rosastr. 9, D-78 Freiburg, W-Germany

ABSTRACT

Fracture phenomena due to internal stresses in toughened glass plates are described. Compared with uniform stress fields a different crack propagation and branching behaviour is observed which can be explained formally by an effective crack length of the order of the plate thickness. The influence of internal stresses on the crack front curvature is shown and a method to measure the K-distribution along the crack front is proposed.

KEYWORDS

Internal stresses, residual stresses, toughened glass, effective crack length, crack front curvature, K-distribution, slow crack propagation, branching.

INTRODUCTION

Internal or residual stresses can influence brittle fracture processes very strongly as for instance in glass. Depending on their magnitude and distribution an extremely different failure behaviour can arise, e.g. very slow crack propagation can lead to final failure after a long time, or a rapid shattering can destroy the component immediately as known from safety glass. Some of these phenomena will be described in this paper and the principles behind these phenomena will be discussed.

For simplification plates are considered containing stress distributions which vary only through the thickness and which are symmetrical to the center plane. Such distributions can be obtained by thermal or chemical treatment of glass plates. In the case of thermal toughening, a parabolic distribution with compression in thick surface layers and tension inside is achieved where the amount of the maximum pressure at the surface is twice as high as the maximum tension in the center plane. In the case of chemical toughening the plates contain a distribution with very high pressure in thin surface layers and low, nearly constant tensile stresses in the large remaining inner part. The cracks considered are through-cracks which propagate in planes perpendicular to the plate surfaces.

PRINCIPAL CONSIDERATIONS

In order to discuss the distribution of the stress intensity factor K along the

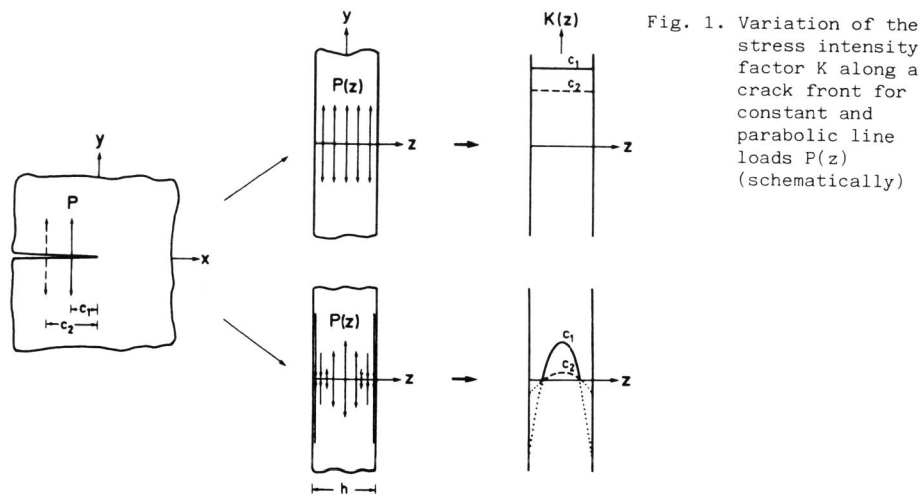


Fig. 1. Variation of the stress intensity factor  $K$  along a crack front for constant and parabolic line loads  $P(z)$  (schematically)

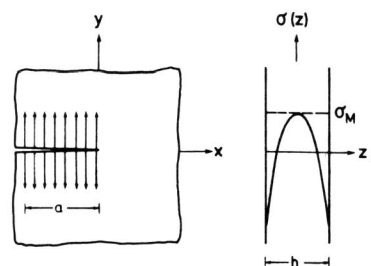


Fig. 2. Stress intensity factor  $K$  in the center of a plate versus relative crack length for different levels  $\sigma_{M_i}$  of uniform (---) and residual (—) stress fields (schematically)

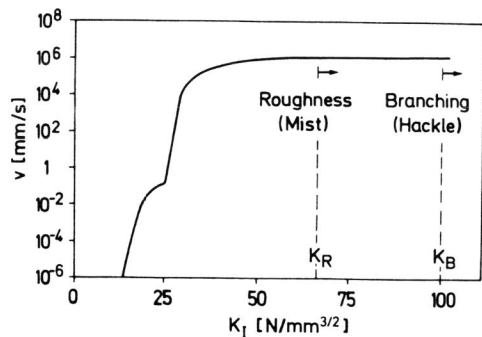
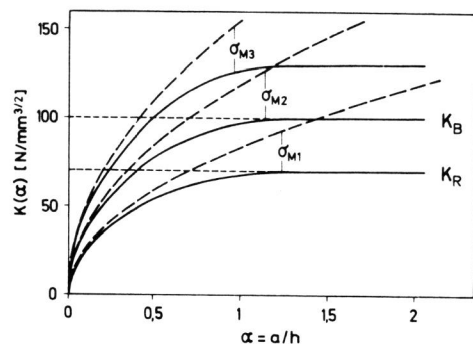


Fig. 3. Crack velocity  $v$  in dependence on the stress intensity factor  $K_I$  (for soda lime silica glass)

crack front caused by the internal stress field a stepwise application of the principle of superposition will be used. It will be assumed that the residual stress field can be considered as the integral of line loads acting directly at the crack surfaces and showing a parabolic distribution. Therefore, as a first step, the effect of single pairs of line loads  $P(z)$  applied to both crack surfaces in the distance  $c_1$  from, but parallel to the straight crack front is discussed. Fig. 1 shows the comparison of a constant line load with one of a parabolic distribution. The following differences in the resulting  $K$ -distributions will be observed. Neglecting the outcome of refined numerical 3D-FE-calculations the constant load leads to a constant  $K$  along the crack front. Since  $K \propto P/\sqrt{c}$  the  $K$ -value will decrease with increasing distance  $c$  according to the given  $1/\sqrt{c}$  proportionality - as it is illustrated by  $c_2$  in Fig. 1. -. In comparison the parabolic load, which represents the thermally produced residual stress field and which fulfills the condition of equilibrium  $\int P(z)dz = 0$ , causes an approximately parabolic  $K$ -distribution along the crack front (Westmann, 1973; Riedmüller, Sommer and Winkler, 1977). Because each part of the line load contributes to the  $K$ -value at any arbitrary point along the crack front, the effect of the tensile forces will be compensated partially by the compression forces weighted by their distance from the point under consideration. Thus, the resulting  $K$ -distribution - especially in the center of the plate - will be considerably lower than that caused by a constant line load of the same maximum magnitude. As a consequence of this effect of compensation a significant  $K$ -distribution will result only for distances  $c$  smaller than the plate thickness.

According to the principle of superposition the  $K$ -distribution for a crack subjected to the complete stress field will be achieved by integrating a sequence of line loads over the whole crack length  $a$  (Fig. 2). For uniform constant stresses the well known dependence  $K \propto \sigma\sqrt{a}$  results which is illustrated in the diagram of Fig. 2 for three different stress levels by dotted curves. However, in the case of the residual stress field the parabolic line loads will mainly contribute to the integral only as long as the distance  $a$  remains small compared to the plate thickness. Therefore, the  $K$ -distribution will increase with  $a$  only for small crack lengths and then remain constant for longer cracks. This is illustrated in the diagram of Fig. 2 by the solid curves which show this behaviour schematically for the  $K$ -value in the plate center again assuming three different levels of residual stresses. The maximum tensile stresses in the center are assumed to be equal to those of the uniform stresses discussed before. These curves demonstrate clearly that for small crack lengths the  $K$ -distribution will be a function of the crack length and the stress level, whereas for cracks exceeding a certain "effective" length on the order of the plate thickness,  $K$  will be a function of the stress level only.

As a result of this effect, pronounced differences in the propagation behaviour of cracks subjected to inhomogeneous internal stresses or uniform external stresses would be expected. Normally the increase of the crack velocity  $v$  is governed by an increase of the stress intensity factor  $K$  according to the well known experimentally established curve shown in Fig. 3 (Wiederhorn, 1967; Richter, 1974). Characteristic values of  $K$  can be attributed to typical changes in the fracture appearance as the onset of slight roughness  $K_R$  or branching  $K_B$ .

On the basis of these considerations the fracture phenomena caused by residual stress fields of different distributions and magnitudes will be explained in the following sections. The first section describes the fracture behaviour in the range of high velocities where branching occurs. The second section deals with relatively slow propagating cracks and in the third section the effect of the inhomogeneous  $K$ -distribution through the thickness on the crack front curvature is discussed.

#### BRANCHING EFFECT

In glasses cracks running with the maximum velocity will branch at a  $K$ -value  $K_B$  which is about four times greater than  $K_{Ic}$  (see Fig. 3). A crack propagating in a

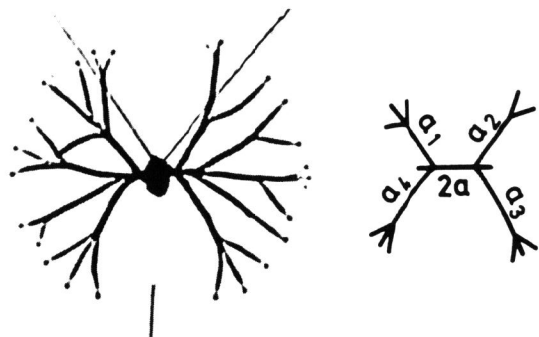


Fig. 4. Crack branching in toughened glass. High speed photography on the left, notation on the right side.

uniform stress field will in every case exceed this value  $K_B$  and will branch according to the stress level at different crack lengths

$$a_B \propto K_B^2 / \sigma^2 \quad (1)$$

as it is illustrated for three different levels in Fig. 2 by the dotted curves. Opposed to this a crack in a residual stress field will exceed  $K_B$  only if the stresses are high enough; for instance  $\sigma_{M3}$  in Fig. 2. For low stresses, such as  $\sigma_{M1}$  no branching will occur, and a limiting stress level  $\sigma_{M2}$  should exist at which  $K_B$  will just be reached.

This branching behaviour has been demonstrated experimentally by initiating center cracks in thermally toughened square plates (300 mm x 300 mm) of different thickness and with different stress levels. The crack usually branches symmetrically at a certain length  $2a$ , such as shown in Fig. 4. The new generated cracks branch again at approximately equal lengths which are denoted by  $a_i$ . In Fig. 5 the measured initial crack lengths are plotted versus the inverse square of the maximum tensile stress in the plate center. The results in Fig. 5 show that for high stress levels the branching behaviour in residual stress fields can be approximately described by the same proportionality as in uniform stress fields according to relation (1); i.e. for low  $\sigma_M^{-2}$  they can be fitted by a line. For lower stresses - varying with the plate thickness - this dependence is no longer valid and a large scatter is observed. For  $h = 6$  mm a well defined limiting stress can be determined which is obviously higher than those which can be estimated for  $h=8$ mm and 10mm.

Since the limiting stresses for  $h=8$ mm and 10mm cannot be determined accurately enough from the data, they are calculated from the data for 6mm. For this purpose all data points which have been used to calculate the single regression lines in Fig. 5, are combined - assuming a similar behaviour for the different thicknesses - and only one least square fit is made shown in Fig. 6. Assuming furthermore for the sake of simplification that the limiting stress depends on the thickness by  $\sigma \propto 1/\sqrt{a_B} \propto 1/\sqrt{h}$ , the limits for  $h=8$ mm and 10 mm are computed from that for 6mm and drawn in Fig. 6 as vertical dotted lines. Their points of intersection with the regression line define formally "effective" crack lengths; i.e. the maximum lengths up to which the K-value depends on the crack lengths. Longer cracks are then controlled by a constant K which may vary locally due to slight imperfections in the toughening process.

A comparable behaviour can be shown for the secondary cracks. The mean values of the crack lengths  $a_i$  (compare Fig. 4) measured in 6mm thick plates are plotted in Fig. 7 in the same manner as before. In Fig. 8 all results for different thicknesses are combined and following the same procedure, but with  $\bar{a}_i$  instead of  $2a$ , the "effective" crack lengths are determined. The resulting values are practically equal to those in Fig. 6 (note that the double values are represented there). In

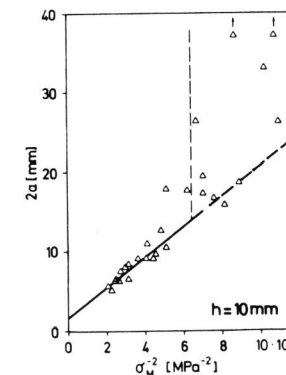
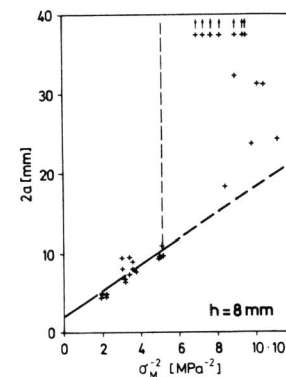
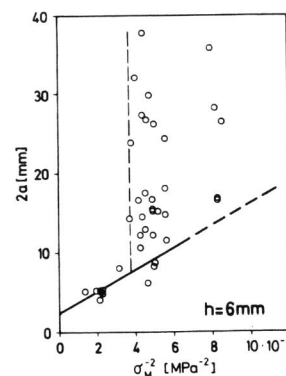


Fig. 5. Crack length  $2a$  at first branching versus  $1/\sigma_M^2$  for different plate thicknesses  $h$  ( $\sigma_M$ : maximum tensile stress in the plate center)

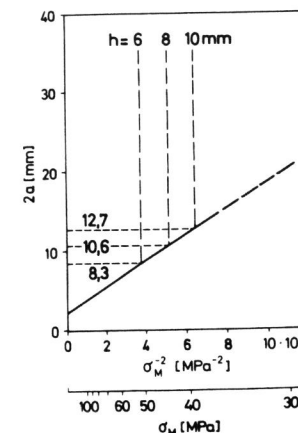


Fig. 6.  $2a$  versus  $1/\sigma_M^2$  using data from all thicknesses; resulting effective crack lengths

summary an "effective" crack length of .7 - .8 h results from all branching experiments in such parabolic stress distributions.

If the stresses are distinctly lower than the limits only single cracks without branching are observed which propagate with high but nearly constant velocity. This was verified by measuring the velocities with the ultrasonic modulation technique (Kerkhof, 1970). It can also be demonstrated clearly by the resulting fracture surfaces. Whereas in a uniform stress field the surfaces are as smooth as a mirror at the beginning and then show roughness, hackling and finally branching with increasing crack length (compare Fig. 9 upper part), in residual stress fields these surfaces are smooth or equally rough in the center over the whole length. This is illustrated in the lower part of Fig. 9 where the roughness even decreases (due to a change in the stress level) despite of increase in crack length.

#### SLOW CRACK PROPAGATION PHENOMENA

A similar propagation behaviour with constant velocity should also be found for the lower velocity range. In this case, however, boundary influences must be taken into account which were neglected for the rapid cracks with lengths small compared with the specimen dimensions. As an example center cracks in square plates are considered again. In this

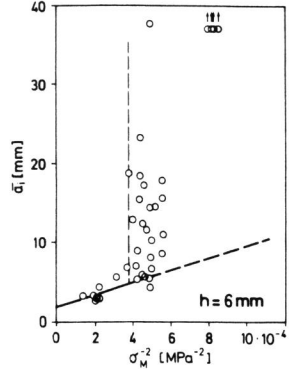


Fig. 7. Mean secondary branching length  $\bar{a}_i$  versus  $1/\sigma_M^2$  for 6mm thick plates

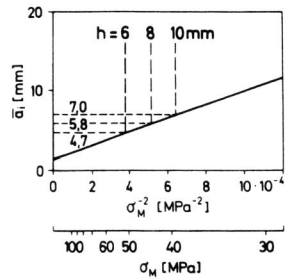


Fig. 8:  $\bar{a}_i$  versus  $1/\sigma_M^2$  using data from different thicknesses; resulting effective crack lengths

case, however, the stress distributions, which are shown schematically in Fig. 10, result from a chemical toughening process. These plates were given the same treatment and therefore exhibit equal compression layers. But since the thicknesses vary, equilibrium requires that the magnitudes of the tensile stresses inside are different. In Fig. 11 the variation of the crack velocity with the relative crack length  $a/v$  for a plate width  $w$  of 100 mm is drawn for three stress levels  $\sigma_M$ . At first, this figure seems to establish a strong dependence on  $a$ . If an estimation is made using the relation for uniform stress fields  $K = \sigma \sqrt{\pi a}$  and the real crack lengths,  $K$ -values result, however, which should be accompanied by much higher velocities up to the maximum ones. Otherwise, using the  $v$ - $K$ -curve of Fig. 3 as a calibration curve the real  $K$ -variation with  $a/w$  can be determined. This is depicted in Fig. 12. It can be seen that  $K$  varies by only about 25% from small

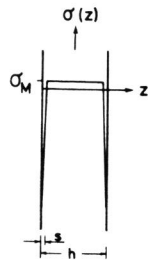


Fig. 10. Stress distribution in chemically toughened glass (schematically)

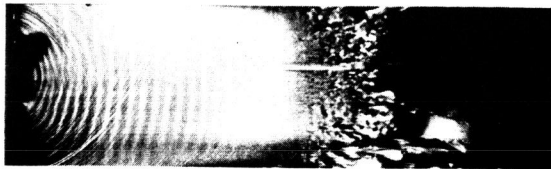


Fig. 9. Crack surfaces in uniform (on the left) and parabolic stress fields (below) at the maximum velocity

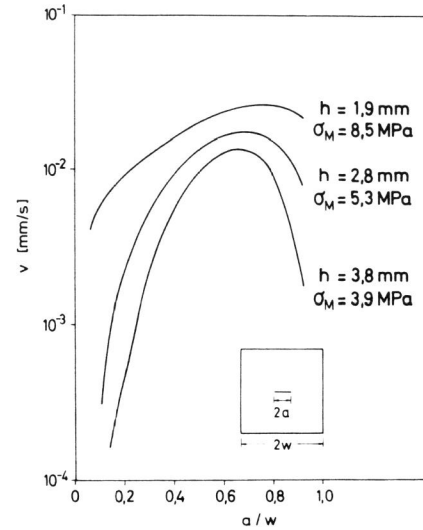
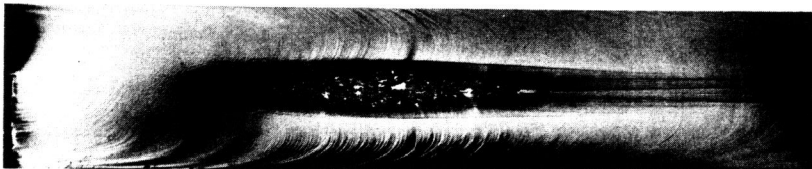


Fig. 11. Crack velocity  $v$  versus relative crack length  $a/w$  in chemically toughened plates with different thicknesses and stresses

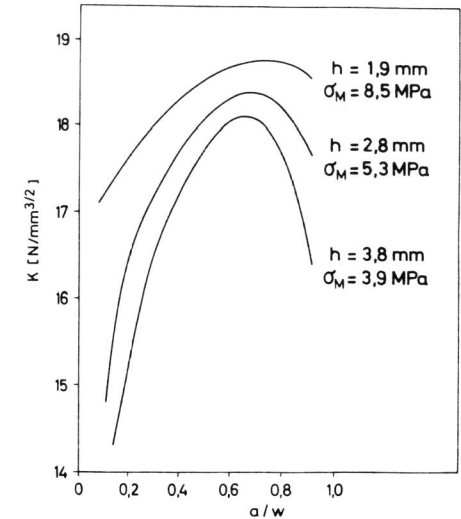


Fig. 12. Stress intensity factors  $K$  in the center plane resulting from Fig. 11

crack lengths up to  $a/w = .6$ . This change can be explained by boundary influences alone (see e.g. Paris and Sih, 1965, who state a correction factor of 1.33 for  $a/w = .6$  for uniformly loaded center cracks), so that in this case the propagation is also governed by a constant effective crack length which can be estimated again to be in the range of  $h$ .

CRACK FRONT CURVATURE AND  $K$  - DISTRIBUTION

Due to the inhomogeneous  $K$ -distribution through the thickness the front of cracks propagating in residual stress fields show a pronounced curvature compared with fronts resulting from a uniform stress field. Figs. 13 and 14 give examples for the slow propagation range; the same specimens as in the section before are considered (compare Figs. 10 - 12). In order to evaluate the local  $K$ -distribution experimentally the real local crack velocities  $v_n$ , normal to the crack front have been determined; these follow from the integral velocity  $v_0$  as shown in Fig. 15. Again using the  $v$ - $K$ -dependence (Fig. 3) as a calibration curve, the corresponding  $K$ -distributions for the four examples under consideration are plotted in Fig. 16. Whereas the crack in the uniform stress field shows an almost constant  $K$ ,  $K$  decreases for the cracks in the residual stress fields from the center to the surface and shows an especially strong decay in the region of the compression layer  $s$ .

Although these results seem to be reasonable, the applicability of the evaluation method may be limited. The calibration curve is established for values of  $v$  and  $K$  averaged over the plate thickness for cracks in uniform stress fields and thus does not exactly represent the local dependence between crack velocity and energy release.

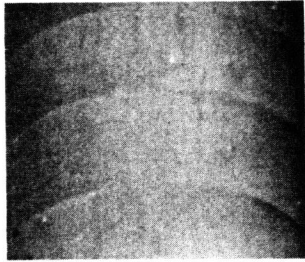


Fig. 13. Crack fronts at slow propagation in a chemically toughened plate; marked by slight pulses

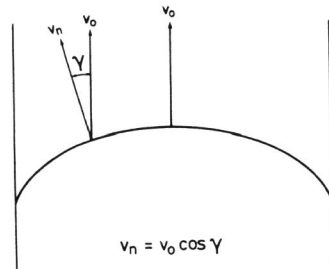


Fig. 15. Relation between the integral crack velocity  $v_0$  and the local velocity  $v_n$  normal to the front

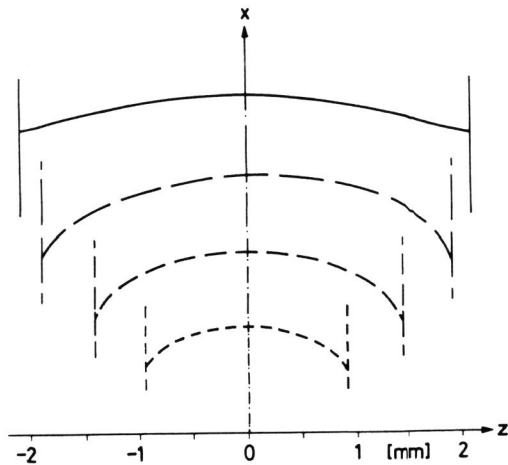


Fig. 14: Crack front curvature in a uniform stress field (on the top) and in chemically toughened plates of different thickness ( $v = 1,2 \cdot 10^{-2}$  mm/s)

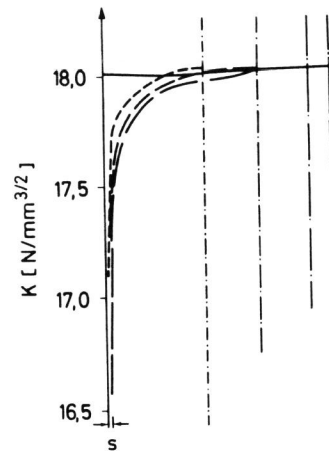


Fig. 16. K-distribution along the crack fronts shown in Fig. 14

#### REFERENCES

- Kerkhof, F. (1970). Bruchvorgänge in Gläsern. Verl. Dtsch. Glastechn. Ges., Frankfurt/M.
- Paris, P.C., and G.C. Sih (1965). Stress analysis of cracks. ASTM STP No. 381
- Richter, H. (1974). Experimentelle Untersuchungen zur Rißausbreitung in Spiegelglas im Geschwindigkeitsbereich  $10^{-3}$  bis  $5 \cdot 10^3$  mm/s. Inst. f. Festkörpermechanik, Freiburg, Bericht 9/74
- Riedmüller, J., E. Sommer and S. Winkler (1977). Die Auswirkungen von Eigenspannungen auf den Spröbruch. Inst. f. Festkörpermechanik, Freiburg, Bericht W 1/77
- Westmann, R. (1973). Private communication